

Spatial Distribution of Naturally Occurring Radioactive Materials in Soil and the Consequent Population Effective Dose

*Habu Tela Abba and Muhammad Sani Isa

Received 20 September 2019/Accepted 29 November 2019/Published online: 30 December 2019

Abstract Protection and assessment of any radiation pollution resulting from the use and disposal of radioactive materials to the large extent is based on the knowledge of natural radioactivity levels of an environment. Therefore, this work was designed to determine the distribution of naturally occurring radionuclides materials (NORMs) (in some residential areas within plateau state). Concentrations of ^{226}Ra , ^{232}Th and ^{40}K in soil across the eight geological formations of Jos Plateau were measured using high resolution HPGe detector. The activity of ^{226}Ra varied between 34 ± 1 and $1006 \pm 18 \text{ Bq kg}^{-1}$, 67 ± 2 and 1695 ± 37 for ^{232}Th and between 67 ± 4 and $2465 \pm 45 \text{ Bq kg}^{-1}$ for ^{40}K . The mean concentration exceeded their corresponding global average values. Annual effective dose due to gamma radiation for general public were within the permissible limit of 1 mSv. The radiometric data obtained from the study could be useful for geochemical exploration in the study area.

Keywords: Spatial distribution; NORMs; geological formation; geostatistical analysis.

*Habu Tela Abba

Department of Physics, Yobe State University, Damaturu, Nigeria

Email: htelaabba@gmail.com

Orcid id: 0000-0003-0842-2235

Muhammad Sani Isa

Department of Physics, Yobe State University, Damaturu, Nigeria

Email: almasmuhammad009@gmail.com

Orcid id: 0000-0002-0377-439X

1.0 Introduction

Living organisms are continuously exposed to a substantial amount of gamma radiation dose as much as 1 Sv due to natural radioactivity mainly from naturally occurring radioactive materials (NORMs), whose origin is often called terrestrial sources (Jibiri, 2001). Natural radioactivity in the environment are derived

from two sources. Firstly, the terrestrial sources from the decay series of primordial radionuclides, associated with ^{238}U and ^{232}Th and the non-decay series of ^{40}K . The second class include those from cosmic radiation. The former are distributed in varying concentration in all types of soil, rocks, plants, sand and water which are significantly influenced by local geology and rainfall of a particular region (Faanu *et al.*, 2013; UNSCEAR, 2000a). Granitic type of igneous rocks have been reported to present higher radioactivity due to its substantial content of radioactive materials such as thorite, monazite and trace amounts of xenotime and rutile compared to limestone, gypsum and chalk which are of sedimentary origin (UNSCEAR, 2008). The distribution of natural radionuclides has been reported by various research work to be associated with the mineral composition of geological makeup and geographical condition of a particular region (Ike *et al.*, 2002a; Jibiri and Ajao, 2004; Tzortzis *et al.*, 2003).

Global increase in energy demand and technological advancements have significantly increase disposal of radioactive materials through transportation and other activities. The risk of abuse and accidents are also high, consequently our natural environment is becoming more vulnerable to pollution by radioactive sources due to anthropogenic activities. Specially, for most cities in Nigeria, comprehensive information on the levels of distribution of natural radioactive materials have not been reported. According to Jibiri (2001), levels of natural radioactivity in Nigeria has not been established and no attempt has been reported on extensive measurement program. Therefore, the present study is aimed at determining spatial distribution pattern of natural radioactive materials in soil across the eight geological formations of Jos Plateau.

2.0 Materials and method

2.1 The Study Area

The study area is located in Jos Plateau in the north central region of Nigeria between the latitudes of $8^{\circ}30'$ - $10^{\circ}24'$ north of the equator

and between longitudes of $9^{\circ}20'$ and $9^{\circ}30'$ of Greenwich meridian. The study area and covers nine local government areas (LGAs) of Plateau state. It has a total land mass area of 15,038 km² and a population of 1,933, 505 (NPC, 2006).

2.2 The geology of the area

Jos plateau is made of eight geological types classified under three geological groups namely; the basement complex, younger granites and volcanic rocks (Falconer, 1921). About 50% of Jos Plateau is underlain by basement complexes such as migmatite-gneiss-quartzite, in some places the basement complex is intruded by Precambrian to the late Paleozoic Pan-African granite (Older Granite), diorite, charnockite. Intrusions of younger granites is also associated with the basement complex (Falconer, 1921). Volcanic rocks such as basalts and rhyolites are found to overlie or cut across the younger granites formation as well as the basement complex. According to Macleod *et al.* (1971), the volcanic rocks were formed during the Tertiary period (Older basalts) and

Quaternary period (Newer basalts). The geological types and their composition are basement complex (G1) (which is composed of metamorphosed Pre-Cambrian sedimentary and volcanic rocks), fine and medium grained biotite (G2) (which is composed of dark phyllosilicate mica mineral and medium-grade metamorphic rock), Older granites (G3), (composed of felsic acidic intrusive igneous rock), rhyolite (G4) (composed of fine-grained porphyritic igneous rock that is dominated by phenocrysts (60%) and quartz (40%) in groundmass, older basalt of Jos (G5)(composed of fine-grained igneous rocks), new basalts (G6)(composed of cones and lavas flows of basaltic scoria (clay) and pyroclastics overlaid by a thick cap of lateritic ironstone. Sandstone, sandy clay and shale (G7) (composed of medium to coarse grained sandstone covered by sediments) and younger granites (G8) (composed of coarse grained biotite, microgranites and some basic rocks. Digitalised map of the geological formations is shown in Fig. 1.

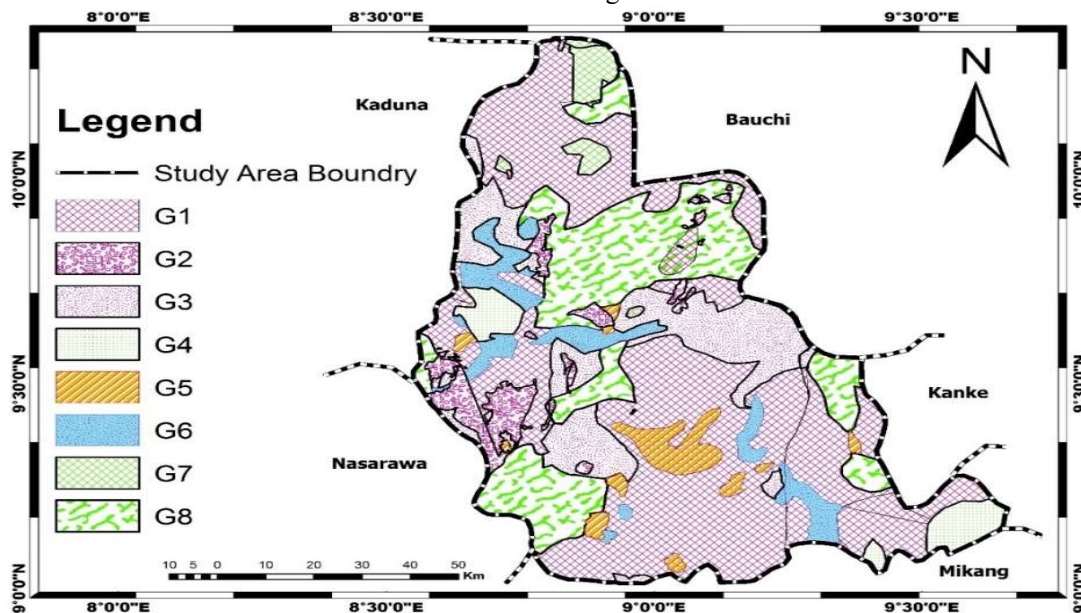


Fig. 1: Geological map of the study area showing different formations

2.3 Soil sampling and preparation

A total of 102 surface soil samples (at a depth of 10 cm) were collected across the geological formations and away from public structures to avoid contribution from non-natural sources using soil sampler. Each sample was packed into a respective sampling polyethylene bag that were firmly tied (and properly labelled to

avoid cross contamination of samples) and stored for further processing. Sampling points were recoded with GPS (Fig. 2). Unwanted materials were removed from the samples including stones, weeds, organic matter and other debris. The prepared samples were, oven dried at 105 °C to a constant weight before grinding. Fine powder of each was packed in



cylindrical containers of uniform size which suited the optimal soil mass of 350 g for the spectrometric analysis of bulk soil samples (Ibeanu, 2003). These containers were sealed and stored for 30 days in order to allow radium and its short-lived daughters to reach secular

equilibrium prior to gamma spectroscopy analysis. Identical containers were also used to pack IAEA reference materials (RGK-1, RGTh-1, and RGU-1) sealed and stored as described previously.

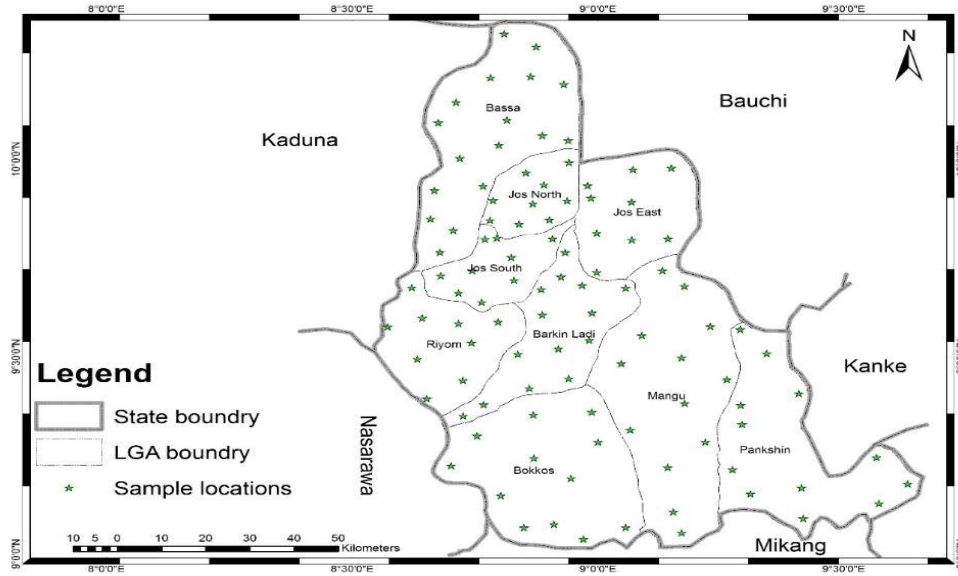


Fig. 2: Soil sampling locations

2.4 Gamma spectrometry analysis

The specific activity concentration for each radionuclides was calculated using equation 1 (Saleh et al., 2013a)

$$A_c = \frac{S}{t_a} + \frac{100}{\epsilon_i} + \frac{100}{y} + \frac{1}{q} \times k \quad (1)$$

where A_c is specific activity concentration of the radionuclide, S is the net area of the peak, t_a is the live time in second, ϵ_i is the efficiency in percentage for the energy line considered, y is the absolute transition probability of the specific gamma ray.

2.5 Radiological risks assessment

2.5.1 Radium equivalent

Radionuclides are not uniformly distributed in soil, radium equivalent (Ra_{eq}) is defined to compared the activities of a material that contains different amount of ^{226}Ra , ^{232}Th and ^{40}K . It is assumed that 259 Bq kg^{-1} of ^{232}Th , 370 Bq kg^{-1} of ^{226}Ra and 4810 Bq kg^{-1} of ^{40}K produce the same γ - rays dose rate in air. Radium equilibrium is computed using the relation given by (Beretka and Mathew, 1985).

$$Ra_{eq} = ^{226}Ra + 1.43 ^{232}Th + 0.077 ^{40}K \quad (2)$$

2.5.2 Absorbed Dose

$$= \text{Doserate}(\text{nGyy}^{-1}) \times 24(\text{h}) \times 365(\text{days}) \times 0.2 \times 0.7 \text{Svy}^{-1} \times 10^{-6} \quad (4)$$

Since gamma radiation dose rates is mainly from the activity concentrations of the radionuclides ^{226}Ra , ^{232}Th and ^{40}K in soil. From the activity concentrations of ^{238}U , ^{232}Th and ^{40}K , gamma dose rate in air was computed using equation 3 (under assumption of uniform distribution of the radionuclides.

$$\text{Absorbed dose} = 0.463 \times A_U + 0.604 \times A_{Th} + 0.417 \times A_K \quad (3)$$

where 0.465, 0.604 and 0.417 are gamma dose conversion coefficients for ^{238}U , ^{232}Th and ^{40}K , respectively (Jibiri and Bankole, 2006).

2.5.3 Annual effective dose

To estimate the annual effective dose outdoor, two factors were considered. The first was is the factor (0.7 Sv Gy^{-1}) that convert absorbed dose in air (nGy h^{-1}) to human effective dose rate (mSv y^{-1}), and the second factor (0.2) gives the time proportion for which an individual is exposed to outdoor radiation (UNSCEAR, 2000a). The annual effective dose (AED) was estimated using the following relation (equation 4).



2.5.4 Collective effective dose

$$\text{Collective effective dose (SC)} = AED \times N(P) \tag{5}$$

where, N(P) is the total population in the study area. Assuming the over 1.9 million population leaving in the area are uniformly exposed to gamma radiation of natural sources. The number of individuals at risk of incurring fatal cancer annually in the area was estimated according to equation 6 (Jibiri, 2001).

$$G = R_F \times SC \tag{6}$$

where G is the number of people to be inflicted by fatal cancer, SC is the collective dose equivalent for the population and R_F is the risk factor and is given as 1.65×10⁻² Sv⁻¹ (NCRP, 1976).

2.6.4 Geostatistical analyses

The data set on the activity concentration of terrestrial radionuclides plus the coordinates for all data points were used in plotting digital maps for the spatial distribution of ²²⁶Ra, ²³²Th and ⁴⁰K for the area. The geostatistical data analysis was performed using a mapping software ArcGIS (version 10.3) (ESRI, 2011). Ordinary Kriging interpolation method for its advantages over other interpolation methods, was chosen. Kriging geostatistical technique interpolate based on the theory of regionalized variables which states that observations close to each other shows spatial

Collective effective dose for the general public was also estimated using equation 5 (ICRP, 1991)

autocorrelation and are more alike than those that are far apart (Matheron, 1963). The technique is unbiased method of interpolation which operate based on the Semivariogram function as defined in equation 7.

$$\gamma(h) = \frac{1}{2N(h)} \sum_{i=1}^{N(h)} \{Z(X_i) - Z(X_i + h)\}^2 \tag{7}$$

where $\gamma(h)$ represent the Semivariogram, $N(h)$ is the number of sample points $Z(X_i)$ is the value of activity concentration of the radionuclides or dose rate measured at sample position X_i , h is the distance between the sample points.

3.0 Results and discussion

3.1 Radioactivities of ²²⁶Ra, ²³²Th and ⁴⁰K

The summary of statistics of the activity concentrations of the natural terrestrial radionuclides ²²⁶Ra, ²³²Th and ⁴⁰K in soil samples obtained using Statistical Package for Social Science (SPSS) software are given in Table 1. The activity concentration of ²²⁶Ra varied from 34±2 to 1006±8 Bq kg⁻¹, 16±1 to 1695±37 for ²³²Th and from 67±4 to 2465±45 Bq kg⁻¹ for ⁴⁰K, with mean values of 186±15, 627±39 and 1056±57 Bq kg⁻¹, respectively.

Table 1: Descriptive statistics of the activity concentration of ²²⁶Ra, ²³²Th and ⁴⁰K

Statistics	²²⁶ Ra (Bq kg ⁻¹)	²³² Th (Bq kg ⁻¹)	⁴⁰ K (Bq kg ⁻¹)
Mean	186	627	1056
Std. Error of mean	15	39	57
Std. Deviation	152	401	580
95% confidence interval of mean	156-215	548-705	942-1169
Median	140	591	964
Minimum	34	16	67
Maximum	1006	1695	2465
Geometric mean	148	472	858
Harmonic mean	121	265	598
Range	34-1006	16-1695	67-2465
Kurtosis	9.73	-0.18	-0.51
Std. error of kurtosis	0.47	0.47	0.47
Skewness	2.75	0.69	0.40
Std. error of skewness	0.23	0.23	0.23
Freq. distribution	Log-normal	Normal	Normal

The activity concentrations of ²²⁶Ra, ²³²Th and ⁴⁰K for each local government areas (LGAs) in the study area is presented in Table 2. The highest activity of ²²⁶Ra and ²³²Th were measured in Bokokos and Barkin Ladi LGAs, respectively

whereas highest mean activity of ⁴⁰K was observed in Jos South. The mean values were distinctly higher than the corresponding world reference values of 35, 40 and 400 Bq kg⁻¹ for ²²⁶Ra, ²³²Th and ⁴⁰K, respectively (UNSCEAR,



2000b). These results are used to evaluate radiological health risk parameters for the area.

Table 2: Activity concentration of radionuclides in soil samples for each L.G.A

LGA	N	²²⁶ Ra (Bq kg ⁻¹)		²³² Th (Bq kg ⁻¹)		⁴⁰ K (Bq kg ⁻¹)	
		Mean	Range	Mean	Range	Mean	Range
Barkin Ladi	16	287±5	67-516	1096±15	610-1627	1210±13	699-1887
Bassa	15	166±3	99-297	568±7	311-1183	1086±15	595-1494
Bokkos	8	356±2	93-1006	829±4	199-1415	1583±5	927-2352
Jos East	9	139±4	91-245	446±6	280-738	744±6	327-1152
Jos North	15	141±3	57-194	611±7	250-1361	922±8	307-1545
Jos South	9	241±5	48-494	923±6	227-1563	1896±12	1492-2465
Mangu	11	123±2	40-291	348±5	38-889	558±4	245-1104
Pankshin	11	99±4	34-253	307±8	16-1090	596±16	67-1672
Riyom	8	164±3	55-487	670±9	67-1695	962±12	248-2188
Overall mean		186	34-1006	627	16-1695	1056	67-2465

3.2 Radium equivalent (Ra_{eq})

The mean Ra_{eq} is estimated to be 1163 Bq kg⁻¹ which is higher than maximum limit of 370 Bq kg⁻¹ to keep annual radiation dose below 1.5 mGy y⁻¹ (Tufail *et al.*, 2006). The observed high concentration of ²³²Th accounts for the measured high value of Ra_{eq}. Indicating that the use of local soil in this area for building materials should be strictly controlled.

3.3 Absorbed dose

Activity concentrations was used to estimate the gamma dose rate for the area. The contribution of each radionuclide is shown in Fig. 3. The Figure

reveals that the largest gamma dose rate (74%) is from ²³²Th while the least (9%) originated from ⁴⁰K. This outcome agrees with the result obtained by Masok *et al.* (2015) in the same region. This is likely linked to the granitic-basement complex formations that constitutes most of the bed rock formations of the region. However, the result is in contrast with lower background areas where ⁴⁰K was found to be higher in concentration at roadsides in high-traffic density areas in Ibadan metropolis, south western Nigeria (Jibiri and Bankole, 2006; Olomo *et al.*, 1994).

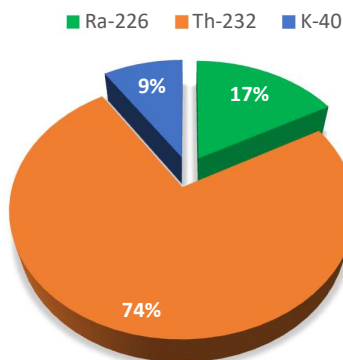


Fig. 3: Contribution of ²²⁶Ra, ²³²Th and ⁴⁰K to dose rate

3.4 Annual effective dose

The values of annual effective dose were estimated to range from 0.065 – 1.95 mSv with a mean of 0.62 mSv. This is much higher than the world average dose equivalent of 0.07 mSv to individuals from gamma radiation dose (UNSCEAR, 2000a).

3.5 Collective dose equivalent

The mean collective effective dose is found to be 1.21×10³ man Sv y⁻¹, which is comparatively

higher than the reference value of 45 man Sv y⁻¹ recommended by ICRP (1991). The result also indicates that 20 people are likely to be inflicted by fatal cancer related diseases every year due to this radiation.

3.6 Isodose maps for the spatial distribution of ²²⁶Ra, ²³²Th and ⁴⁰K

The activities of the terrestrial radionuclides were used to plot a digital maps for the spatial distribution of ²²⁶Ra, ²³²Th and ⁴⁰K for the study



area. Spatial distribution map of ^{226}Ra is shown in Fig. 4. Elevated spots were observed in Bokkos LGA with relatively higher concentration in areas around Mangu, Pankshin and Riyom LGAs. Concentration of ^{232}Th was high in areas around

Jos South, Barkin Ladi and in Pankshin LGAs with the most elevated spot found in Jos South (Fig. 5). Higher activity of ^{40}K was noted in some locations around Pankshin, Mangu and Riyom LGAs as shown in Fig. 6.

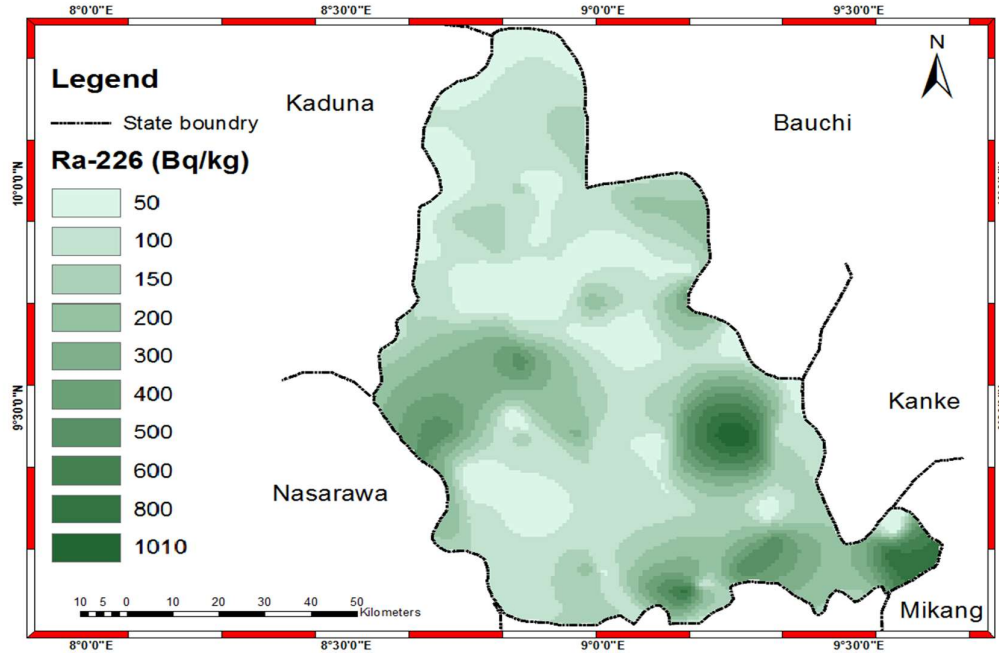


Fig. 4: Spatial distribution map of ^{226}Ra .

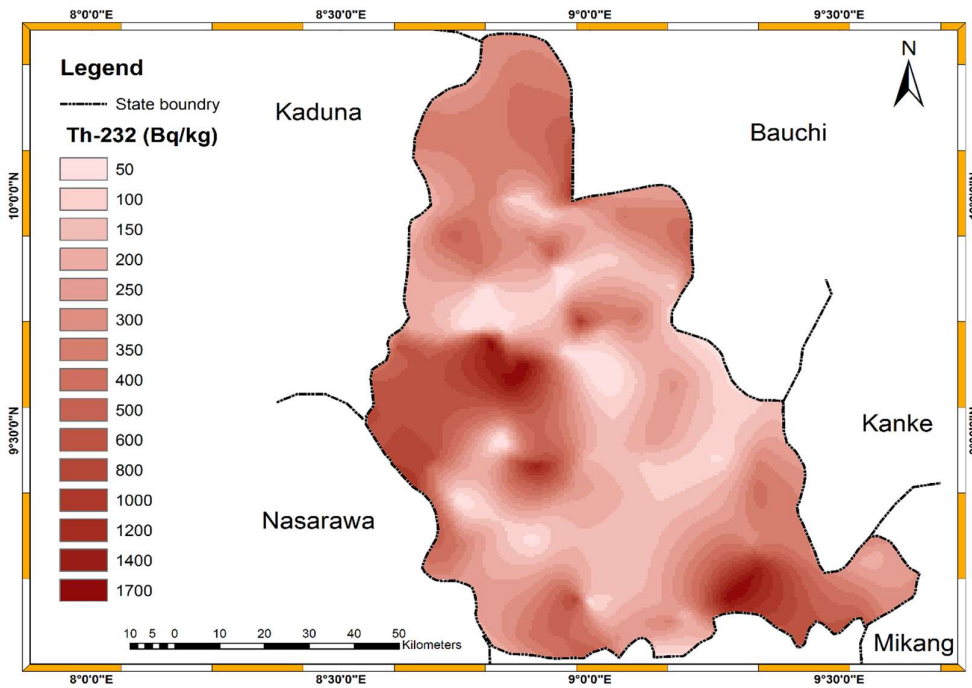


Fig. 5: Spatial distribution of ^{232}Th .



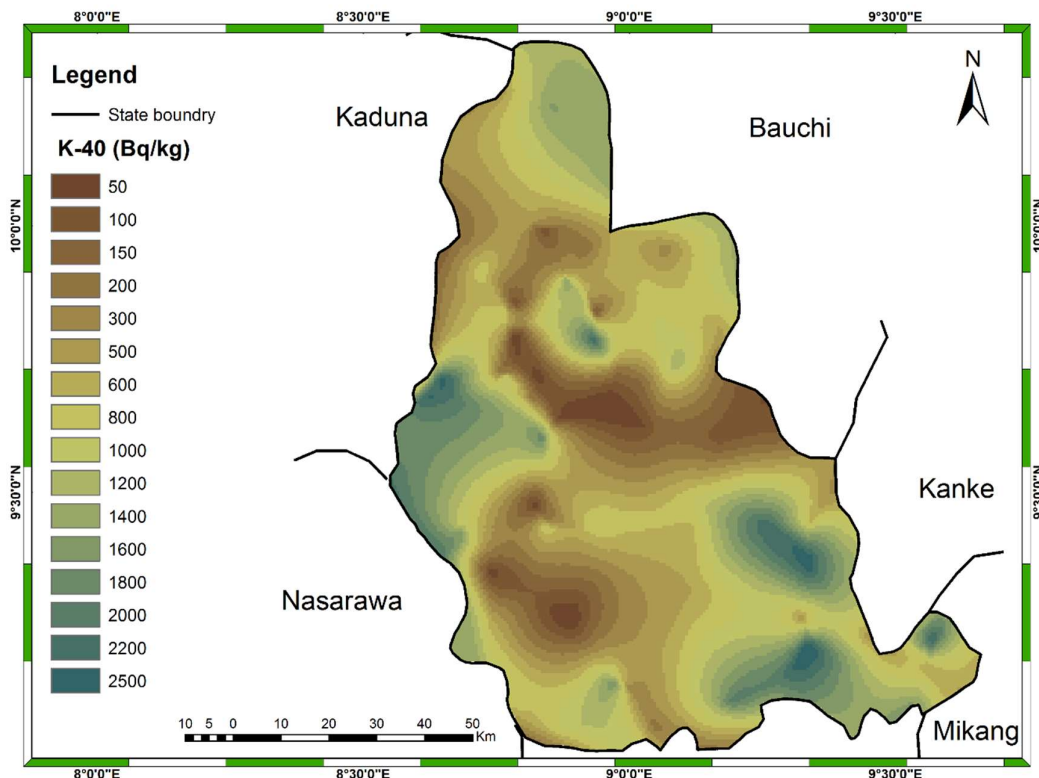


Fig. 6: Spatial distribution of ^{40}K .

4.0 Conclusion

Activity concentrations of NORMs in soil were measured to determine the distribution of ^{238}U , ^{232}Th and ^{40}K in Jos Plateau. The mean activity concentrations were found to be higher than the global average measured for earth crust. ^{232}Th was found to contribute the largest portion (74%) to total radioactivity of the area. The results obtained were used to estimate the gamma absorbed dose and the corresponding annual effective for individuals living in the study area. The results and findings from the study indicated that 20 people are likely to be inflicted by fatal cancer related diseases every year due to natural radioactivity from soil. The maps for the spatial distribution of the radionuclides revealed that elevated concentrations of radionuclides in the study area vary within the LGAs. Therefore, Jos Plateau can be considered as a high background radiation area (HBRA). The results of this work can be used as reference data for ascertaining possible changes in environmental radioactivity due to release from anthropogenic sources. The results can also be useful for radiochemical exploration.

5.0 References

- Beretka, J. & Mathew, P. (1985). Natural radioactivity of Australian building materials, industrial wastes and by-products. *Health physics*, 4, 8, pp. 87-95.
- ESRI, R. (2011). ArcGIS desktop: release 10. *Environmental Systems Research Institute, CA*.
- Faanu, A., Kpeglo, D., Sackey, M., Darko, E., Emi-Reynolds, G., Lawluvi, H., Awudu, R., Adukpo, O., Kansaana, C. & Ali, I. (2013). Natural and artificial radioactivity distribution in soil, rock and water of the Central Ashanti Gold Mine, Ghana. *Environmental Earth Sciences*, 70, 2, pp. 1593-1604.
- Falconer, J. D. (1921). *The geology of the plateau tin fields. authority of the Nigerian government*. Waterlow & Sons, Limited, Nigeria.
- Ibeanu, I. G. E. (2003). Tin mining and processing in Nigeria: cause for concern? *Journal of Environmental Radioactivity*, 6, 4, pp. 59-66.
- ICRP, (1991). ICRP Publication 60: 1990 *Recommendations of the International Commission on Radiological Protection*. ICRU Publication 60, Pergamon Press, Oxford. Elsevier Health Sciences.



- Ike, E. E., Solomon, A. O., Jwanbot, D. N. & Olomo, J., Akinloye, M. & Balogun, F. (1994). Distribution of natural gamma radiation dose rates within the Toro Sheet 148, North Central Nigeria. In: *Zuma Journal of Pure and Applied Sciences*, 4, 1, pp 87-89.
- Jibiri, N. (2001). Assessment of health risk levels associated with terrestrial gamma radiation dose rates in Nigeria. *Environment international*, 2, 7, pp. 21-26.
- Jibiri, N. & Ajao, A. (2004). Natural activities of ^{40}K , ^{238}U and ^{232}Th in elephant grass (*Pennisetum purpureum*) in Ibadan metropolis, Nigeria. *Journal of Environmental Radioactivity*, 7, 8, pp. 105-111.
- Jibiri, N. & Bankole, O. (2006). Soil radioactivity and radiation absorbed dose rates at roadsides in high-traffic density areas in Ibadan metropolis, southwestern Nigeria. *Radiation Protection Dosimetry* 11, 8, pp. 453-458.
- Masok, F. B., Masiteng, P. L. & Jwanbot, D. (2015). Natural radioactivity concentrations and effective dose rate from Jostin mining dumpsites in Rayfield, Nigeria. *Journal of Environmental and Earth Sciences*, 5, 1, pp. 51-55.
- Matheron, G. (1963). *Principles of geostatistics. Economic Geology*, 5, 8, pp. 1246-1266.
- NCRP (1976). *Environmental radiation measurements*. National Council on Radiation Protection and Measurements (NCRP) report no.50.
- NPC (2006). National population Commission (NPC):. *Provisional of 2006 Census Results*. Abuja, Nigeria.
- Distribution of gamma-emitting natural radionuclides in soils and water around nuclear research establishments, Ile-Ife, Nigeria. Nuclear Instruments and Methods in Physics Research Section A: Accelerators, Spectrometers, Detectors and Associated Equipment, 35, 3, pp. 553-557.
- Saleh, M. A., Ramli, A. T., Alajerami, Y., Aliyu, A. S. & Basri, N. A. B. (2013a). Radiological study of Mersing District, Johor. *Radiation Physics and Chemistry*, 8, 5, pp. 107-117.
- Tufail, M., Akhtar, N. & Waqas, M. (2006). Radioactive rock phosphate: the feed stock of phosphate fertilizers used in Pakistan. *Health Physics*, 90, 1, pp. 361-370.
- Tzortzis, M., Tsertos, H., Christofides, S. & Christodoulides, G. (2003). Gamma radiation measurements and dose rates in commercially-used natural tiling rocks (granites). *Journal of Environmental Radioactivity*, 70 1, pp. 223-235.
- UNSCEAR, (2000a). *Sources and effects of ionizing radiation*:. New York: United Nations.,
- UNSCEAR (1993) *Report to the General Assembly with scientific annexes / United Nations Scientific Committee on the Effects of Atomic Radiation*.
- UNSCEAR, (2000b). *Sources, effects and risks of ionizing radiation*. Report to the General. United Nations Scientific Committee on the effects of atomic radiation.. Assembly with annexB, United Nations, New York.
- UNSCEAR, (2008). *Sources and effects of ionizing radiation*. United Nations Scientific Committee on the Effects of Atomic Radiation, New York.

